

# Water-Group Ion Distributions in the Mid-Cometosheath of Comet Halley

D. E. HUDDLESTON, M. NEUGEBAUER, AND B. E. GOLDSTEIN

*Jet Propulsion Laboratory, California Institute of Technology,  
Pasadena, California*

Brief Report

for submission to *Journal of Geophysical Research*

May 1993

## Abstract

In the mid-cometosheath of comet Halley ( $1-2 \times 10^5$  km from the nucleus) the center-of-mass plasma frame is approximately the bulk flow velocity of the cometary ions, and the Alfvén wave speed is an appreciable fraction of the flow speed. Here, the peaks of the water-group ion distributions observed by the Giotto Ion Mass Spectrometer are at velocities consistently below the expected pickup speed. It is shown that this effect is consistent with the scattering of the new pickup ions onto a bispherical shell distribution. The model does not fit the data inside  $\sim 1.2 \times 10^5$  km however, possibly as a result of the growing importance of collisions or the presence of other processes such as scattering on obliquely-propagating magnetosonic waves.

## 1. INTRODUCTION

Volatile cometary material sublimates from the surface of the nucleus and expands to distances of the order of  $10^6$  to  $10^7$  km from the comet. The gas is ionized both by solar photons and as a result of charge exchange with solar wind ions. In the frame of the solar wind the newly born ions are initially injected at speed  $|\mathbf{v}_{\text{inj}}| = u_{\text{sw}}$  the local solar wind speed, with direction antiparallel to  $\mathbf{u}_{\text{sw}}$ . The component of  $\mathbf{v}_{\text{inj}}$  perpendicular to the interplanetary magnetic field,  $\mathbf{B}$ , is very rapidly picked up into a gyration about the field lines due to the Lorentz force, and the implanted ions initially form a ring-beam in velocity space. The ring-beam geometry is determined by the angle,  $\alpha$ , between  $\mathbf{u}_{\text{sw}}$  and  $\mathbf{B}$ . This distribution is unstable to the generation of Alfvén waves [Wu and Davidson, 1972; Galeev, 1986; Sagdeev *et al.*, 1986] with which the pickup ions interact to become scattered from a ring-beam distribution toward a shell-like distribution in velocity space. The likely asymptotic pitch angle distribution is the bispherical shell [Galeev and Sagdeev, 1988; Huddleston and Johnstone, 1992] which comprises the low energy

portions of the characteristic curves centered on the parallel-propagating Alfvén wave velocities  $\pm V_A$ . The geometry of the bispherical shell is illustrated in Figure 1. Development of a bispherical shell is supported by observations of pickup ions near the bow shock at comet Halley [Coates *et al.*, 1990], and also by numerical calculations [Miller *et al.*, 1991; Huddleston *et al.*, 1992].

Neither the existence nor the importance of the bispherical shell distribution has been demonstrated closer to the nucleus where the heavy cometary ions dominate the mass flux and the center-of-mass plasma frame is approximately the bulk speed,  $\mathbf{u}_{wg}$ , of the water group ions. In this region, the interplanetary magnetic field is "frozen in" with  $\mathbf{u}_{wg}$  rather than with  $\mathbf{u}_{sw}$ . Another change is that as the magnetic field strength increases in the magnetic pileup region [Neubauer *et al.*, 1986], the Alfvén speed becomes an appreciable fraction of the flow speed. In this paper we explore some of the expected consequences of the bispherical distribution in the mid-cometosheath of comet Halley and use the results to explain some of the features observed by the Ion Mass Spectrometer (IMS) on the Giotto mission at distances from the nucleus of  $\sim 1\text{-}2 \times 10^5$  km.

## 2. OBSERVED DISTRIBUTIONS

The data examined in this paper were obtained by the High Energy Range Spectrometer (HERS) of the IMS on the inbound leg of the Giotto trajectory. A description of the HERS experiment is provided by Balsiger *et al.* [1987] and details of the data reduction techniques are given by Goldstein *et al.* [1992].

Examples of the water-group-ion (ion mass/charge = 16-18 amu/q) phase space density distributions,  $F_{wg}(v)$ , obtained from the IMS HERS are presented in Figure 2. Additional examples are shown in Figure 4 of Goldstein *et al.* [1992]. The distributions are in the frame of their bulk flow velocity  $\mathbf{u}_{wg}$ . The dashed curves in each plot in Figure 2 are (in arbitrary units) the number density of the ions in each spherical shell,

$n_{bin}$ , calculated from the phase space density values by multiplying by the shell volume  $\frac{4}{3}\pi(v_{upper}^3 - v_{lower}^3)$  where  $v_{upper}$  and  $v_{lower}$  are the upper and lower boundaries of the velocity bin. The peaks in both  $F_{wg}(v)$  and  $n_{bin}$  are at significantly lower velocities than the average bulk speed  $|u_{wg}|$  indicated by the arrows in each plot. As the spacecraft approaches the comet, the rate of pickup of newly created ions increases, and we expect the ion distribution function to be dominated by the most recently picked-up ions. If the newest ions are picked up at a relative speed of  $|u_{wg}|$ , why are the peaks of the distributions consistently below  $|u_{wg}|$ , especially in view of an expected bias in the opposite direction caused by the ions picked up earlier at higher flow speeds? We show in the next section that this effect could be a signature of the scattering of ions into a bispherical shell distribution under conditions of the Alfvén speed being a sizable fraction of the plasma flow speed.

Figure 3 shows an example of contours of the velocity distribution function of water-group ions in a magnetic coordinate system centered at the bulk velocity  $u_{wg}$  (from Goldstein *et al.* [1992]). In these coordinates, newly injected ions would first appear at the location denoted by +, and would then scatter along the two spherical sections centered on  $\pm V_A$  that have been superimposed on the contours in Figure 3. Qualitatively, the bispherical shell fits the data reasonably well, especially when one considers that the plasma is decelerating and that the distribution must contain a significant number of ions picked up at higher flow speeds. The comparison between the observations and the bispherical shell model is put on a more quantitative basis below.

### 3. IMPLANTATION SHELL RADIUS

Far from the comet where the solar wind mass density exceeds that of the implanted cometary ion population, newly born ions are injected at  $|u_{sw}|$  and scatter on  $\pm V_A$  in the solar wind frame, toward a bispherical shell distribution. For such a

distribution, the bulk speed in the solar wind frame is field-aligned upstream and lies between 0 and  $V_A$  as has been observed near the bow shock at Halley [Coates *et al.*, 1990]. As the cometary ions begin to dominate and the center of mass frame shifts to  $\mathbf{u}_{wg}$  (this transition occurs slowly, of course), the newly ionized particles experience the motional electric field and Lorentz force in the  $\mathbf{u}_{wg}$  frame, and scatter on  $\pm V_A$  speeds in this new frame. Thus new ions are added onto a bispherical shell that differs from those of the previously assimilated ions, and the bulk flow speed is shifted even further into the upstream direction relative to  $\mathbf{u}_{sw}$ .

Assuming the newly injected ions scatter onto a bispherical shell, the average radius  $\langle |v| \rangle_{inj}$  of the shell relative to the center of the plasma frame (at  $\mathbf{u}_{wg}$ ) may be calculated to estimate the position of the injection peak in the  $F_{wg}(v)$  or  $n_{bin}$  water group distributions. The geometry used in the calculation is shown in Figure 4. The average radius of the shell portion centered on  $-V_A$  is calculated by integrating  $|\mathbf{V}_u + \mathbf{V}_A| = [(V_u \cos \theta + V_A)^2 + (V_u \sin \theta)^2]^{1/2}$  over the shell surface from  $\theta = \theta_u$  to  $\pi$ , where  $\mathbf{V}_A$  is field aligned along  $+v_{||}$  and  $\mathbf{V}_u$  is a vector to  $-V_A$  from a given point on the partial shell surface. Similarly for the  $+V_A$  centered partial shell,  $[(V_d \cos \theta + V_A)^2 + (V_d \sin \theta)^2]^{1/2}$  is integrated from  $\theta = \theta_d$  to  $\pi$ . Note  $\cos \theta_d$  is negative since the initial ring-beam is always upstream along  $v_{||}$  with respect to the bulk flow (see Figure 4); the angle  $\alpha$  between the flow velocity and  $\mathbf{B}$  determines the geometry of the ring-beam in velocity space.

For the upstream-centered partial shell, the average radius from the  $\mathbf{u}_{wg}$ -frame center is given by

$$\langle |v| \rangle_u = \frac{2\pi V_u^2 \int_{\theta_u}^{\pi} [V_u^2 + V_A^2 + 2V_u V_A \cos \theta]^{1/2} \sin \theta d\theta}{2\pi V_u^2 \int_{\theta_u}^{\pi} \sin \theta d\theta} \quad (1)$$

where a uniform distribution of particles over the surface of the partial shell is assumed.

The integration gives

$$\langle |v| \rangle_u = \frac{1}{3V_u V_A (1 + \cos \theta_u)} \left[ (V_u^2 + V_A^2 + 2V_u V_A \cos \theta_u)^{3/2} - (V_u^2 + V_A^2 - 2V_u V_A)^{3/2} \right] \quad (2)$$

$$\langle |v| \rangle_d = \frac{1}{3V_d V_A (1 + \cos \theta_d)} \left[ (V_d^2 + V_A^2 + 2V_d V_A \cos \theta_d)^{3/2} - (V_d^2 + V_A^2 - 2V_d V_A)^{3/2} \right] \quad (3)$$

The  $\langle |v| \rangle_u$  and  $\langle |v| \rangle_d$  expressions are similar in form because  $\theta_u$  and  $\theta_d$  are defined from the upstream and downstream field-aligned directions, respectively, as shown in Figure 4.

The average radius (in the  $u_{wg}$  frame) for the composite bispherical shell is obtained by weighting the above averages according to the relative surface areas of the two shell portions. This assumes full scattering of the newly injected ions onto the bispherical shell in our theoretical approximation. Thus we have

$$\langle |v| \rangle_{inj} = w_u \langle |v| \rangle_u + w_d \langle |v| \rangle_d \quad (4)$$

for the new ions added to the implanted ion distribution, where the weightings are (see also *Huddleston and Johnstone* [1992])

$$w_u = \frac{V_u^2 (1 + \cos \theta_u)}{V_u^2 (1 + \cos \theta_u) + V_d^2 (1 + \cos \theta_d)} \quad (5)$$

$$w_d = \frac{V_d^2 (1 + \cos \theta_d)}{V_u^2 (1 + \cos \theta_u) + V_d^2 (1 + \cos \theta_d)} \quad (6)$$

The injection angles  $\theta_u$  and  $\theta_d$ , and the radii of the upstream- and downstream-centered shell portions in the frame of the  $-V_A$  and  $+V_A$  scattering centers are given in terms of  $u_{wg}$ ,  $\alpha$  and  $V_A$  by geometry:

$$\cos \theta_u = \frac{u_{wg} \cos \alpha - V_A}{V_u} \quad (7)$$

$$\cos \theta_d = \frac{-u_{wg} \cos \alpha - V_A}{V_d} \quad (8)$$

$$V_u^2 = u_{wg}^2 \sin^2 \alpha + (u_{wg} \cos \alpha - V_A)^2 \quad (9)$$

$$V_d^2 = u_{wg}^2 \sin^2 \alpha + (u_{wg} \cos \alpha + V_A)^2 \quad (10)$$

The fractional reduction of the injection radius from  $u_{wg}$  to  $\langle |v| \rangle_{inj}$  in the bispherical shell approximation depends on the ratio of  $V_A$  to  $u_{wg}$  which characterizes the geometry of the bispherical shell. Figure 5 presents curves of  $\langle |v| \rangle_{inj}/u_{wg}$  versus  $\alpha$ , for a set of  $V_A/u_{wg}$  values. For  $V_A \ll u_{wg}$ , the magnitude of the injection radius in the implanted ion frame is approximately  $u_{wg}$ . As  $V_A/u_{wg}$  increases, as is the case where the plasma flow slows and stagnates in the inner coma, then  $\langle |v| \rangle_{inj}$  can be appreciably reduced from  $u_{wg}$  since the theoretical bispherical shell geometry becomes significantly different from a spherical shell. The effect is largest for small  $\alpha$ . It should be noted, however, that the firehose instability may become important for low- $\alpha$  conditions [Galeev *et al.*, 1991] and the bispherical shell approximation is therefore likely to become increasing more inaccurate as  $\alpha \rightarrow 0$ .

To test the bispherical shell model, we have combined values of  $u_{wg}$ ,  $\alpha$ , and  $V_A$  obtained from the observations with Equations (2)-(10) to calculate  $\langle |v| \rangle_{inj}$ . The results are displayed as the dotted curve in Figure 6. The filled circles in Figure 6 are the HERS measurements of  $u_{wg}$  taken from Neugebauer *et al.* [1992], while the dashed line represents a linear fit ( $u_{wg} = 0.0002 D$ ) to the water-group velocities measured by both the HIS and HERS sensors over the distance range  $D = 2000$  to  $300,000$  km from the comet along the inbound Giotto path (data presented by Altwegg *et al.* [1993]). Values of the Alfvén speed are plotted at the bottom of the Figure. The peaks of the  $n_{bin}$

distributions estimated from the observed distributions (see examples in Figure 2) are plotted as X's in Figure 6 with error bars equal to the 6.25 km/s bin widths  $d\nu$  of the distributions. It is seen that these points lie below  $u_{wg}$  and coincide reasonably well with the theoretical approximation in the distance range  $1.2 - 1.8 \times 10^5$  km from the nucleus. Inside  $1.2 \times 10^5$  km, the observed peak radii are closer to  $u_{wg}$  than to  $\langle |v| \rangle_{inj}$ .

#### 4. CONCLUSIONS AND DISCUSSION

We have shown theoretically that when the Alfvén speed is an appreciable fraction of the local plasma speed, the scattering of newly picked-up ions onto bispherical shells can significantly affect the isotropy and the shape of the distribution function, with the peak of the distribution being well below the local ion speed. Quantitative theoretical values are plotted in Figure 5.

The water-group distribution functions are consistent with the bispherical shell distribution in the mid-cometosheath over the distance range  $1.2-1.8 \times 10^5$  km. Water-group ion spectra are not available at greater distances. There are several possible explanations for the break-down of the model inside  $1.2 \times 10^5$  km: (1) The expectation of a bispherical shell distribution is based on the assumption that the ions are scattered by Alfvén waves propagating parallel and antiparallel to the field. In reality, the pickup ions may possibly also scatter on obliquely-propagating magnetosonic waves [Tsurutani, 1991a; Tsurutani, 1991b; Srivastava *et al.*, 1993]. We do not know whether or not obliquely propagating waves became more important inside  $1.2 \times 10^5$  km. (2) Both ion-ion and ion-neutral collisions become increasingly important inside a distance of  $\sim 10^5$  km, and dominate cometary processes by  $10^4$  km [e.g., Puhl *et al.*, 1993]. (3) There may be an effect due to movement of pickup ions across flowlines as they are continuously injected and convected toward the comet, which cannot be accounted for in our theoretical model using locally measured  $V_A$  and  $\alpha$  values to calculate the injection



radius. (4) The observational "points" in Figure 6 each represent averages of a number of distributions obtained along the spacecraft path. (5) If the ion implantation rate becomes very high, the ions do not have time to scatter fully to a shell-like distribution. It is not possible, however, to appeal to the firehose instability to explain the discrepancy at  $1.0\text{-}1.2 \times 10^5$  km because  $\alpha$  was  $>45^\circ$  throughout that region.

A comprehensive model of the interaction of active comets with the solar wind requires correct accounting of not only the injection rate, but also the energy changes of picked up ions. From the present work it appears that newly injected ions initially lose energy in the plasma frame as the result of scattering processes. In future studies we intend to extend the study of the Giotto ion distribution functions to deduce experimental values for parameters such as the ion injection rate, the velocity diffusion rate, and the charge-exchange rate, to deduce other parameters required for such a model.

*Acknowledgments.* This paper represents one aspect of research carried out at the Jet Propulsion Laboratory of the California Institute of Technology under contract to the National Aeronautics and Space Administration. DEH was supported by the Resident Research Associate Program of the National Research Council.

## REFERENCES

- Altwegg, K., H. Balsiger, J. Geiss, R. Goldstein, W.-H. Ip, A. Meier, M. Neugebauer, H. Rosenbauer, and E. Shelley, The ion population between 1300 km and 230,000 km in the coma of comet P/Halley, *Astron. and Astrophys.*, *in press*, 1993.
- Balsiger, H., K. Altwegg, F. Bühler, J. Fisher, J. Geiss, A. Meier, U. Rettenmund, H. Rosenbauer, R. Schwenn, J. Benson, P. Hemmerich, K. Säger, G. Kulzer, M. Neugebauer, B. E. Goldstein, R. Goldstein, E. G. Shelley, T. Sanders, D. Simpson, A. J. Lazarus, and D. T. Young, The Giotto Ion-mass spectrometer, *J. Phys. E.*, *20*, 759, 1987.
- Coates, A. J., B. Wilken, A. D. Johnstone, K. Jockers, K.-H. Glassmeier, and D. E. Huddleston, Bulk properties and velocity distributions of water group ions at comet Halley: Giotto measurements, *J. Geophys. Res.*, *95*, 10249, 1990.
- Galeev, A. A., Theory and observations of solar wind/cometary plasma interaction processes, in: *Proc. of 20th ESLAB Symposium on the Exploration of Halley's Comet*, edited by B. Battrock, E. J. Rolfe and R. Reinhard, *Vol. I*, pp. 3, ESA SP-250, Heidelberg, Germany, 1986.
- Galeev, A. A., and R. Z. Sagdeev, Alfvén waves in a space plasma and its role in the solar wind interaction with comets, *Astrophys. Space Sci.*, *144*, 427, 1988.
- Galeev, A. A., R. Z. Sagdeev, V. D. Shapiro, V. I. Shevchenko, and K. Szego, Quasilinear theory of the ion cyclotron instability and its application to the cometary plasma, in *Cometary Plasma Processes*, edited by A. D. Johnstone, pp. 223, AGU, Washington, D.C., 1991.
- Goldstein, B. E., R. Goldstein, M. Neugebauer, S. A. Fuselier, E. G. Shelley, H. Balsiger, G. Kettmann, W.-H. Ip, H. Rosenbauer, and R. Schwenn, Observations of plasma dynamics in the coma of P/Halley by the Giotto Ion Mass Spectrometer, *J. Geophys. Res.*, *97*, 4121, 1992.

- Huddleston, D. E., A. J. Coates, and A. D. Johnstone, Quasi-linear velocity space diffusion of heavy cometary pickup ions on bispherical diffusion characteristics, *J. Geophys. Res.*, **97**, 19163, 1992.
- Huddleston, D. E., and A. D. Johnstone, Relationship between wave energy and free energy from pickup ions in the comet Halley environment, *J. Geophys. Res.*, **97**, 12217, 1992.
- Miller, R. H., S. P. Gary, D. Winske, and T. I. Gombosi, Pitch-angle scattering of cometary ions into monospherical and bispherical distributions, *Geophys. Res. Lett.*, **18**, 1063, 1991.
- Neubauer, F. M., K. H. Glassmeier, M. Pohl, J. Raeder, M. H. Acuña, L. F. Burlaga, N. F. Ness, G. Musmann, F. Mariani, M. K. Wallis, E. Ungstrup, and H. U. Schmidt, First results from the Giotto magnetometer experiment at comet Halley, *Nature*, **321**, 352, 1986.
- Neugebauer, M., B. E. Goldstein, R. Goldstein, S. A. Fuselier, F. M. Neubauer, and W.-H. Ip, A different view of plasma flow inside P/Halley, *Astron. Astrophys.*, **258**, 549, 1992.
- Puhl, P., T. E. Cravens, and J. Lindgren, Ion thermalization in the inner coma of a comet, *Astrophys. J.*, *submitted*, 1993.
- Sagdeev, R. Z., V. D. Shapiro, V. I. Shevchenko, and K. Szegö, MHD turbulence in the solar wind - comet interaction region, *Geophys. Res. Lett.*, **13**, 85, 1986.
- Srivastava, K. M., B. T. Tsurutani, B. E. Goldstein, V. Sharma, and M. Okada, Acceleration of cometary H<sub>2</sub>O group pickup ions by obliquely propagating nonlinear magnetosonic waves, *J. Geophys. Res.*, *submitted*, 1993.
- Tsurutani, B. T., Comets: a laboratory for plasma waves and instabilities, in *Cometary Plasma Processes*, edited by A. D. Johnstone, pp. 189, AGU, Washington, D.C., 1991a.

- Tsurutani, B. T., Nonlinear low frequency (LF) waves: comets and foreshock phenomena, in *Physics of Space Plasmas*, edited by T. Chang, G. B. Crew and J. R. Jasperse, pp. 91, Scientific Publishers, Inc., Cambridge, MA, 1991b.
- Wu, C. S., and R. C. Davidson, Electromagnetic instabilities produced by neutral particle ionization in interplanetary space, *J. Geophys. Res.*, 77, 5399, 1972.

## FIGURE CAPTIONS

Fig. 1. Sketch of the theoretical bispherical shell geometry for implanted cometary ions in the solar wind frame, where  $v_{\parallel}$  and  $v_{\perp}$  are the field-aligned and perpendicular (gyrating) velocities, respectively. The shell comprises the low energy portions of the ion paths about the scattering centers of the upstream and downstream propagating Alfvén waves,  $-V_A$  and  $+V_A$ , respectively.

Fig. 2. Examples of the cometary water-group ion distributions observed by the Giotto Ion Mass Spectrometer. The solid curves in each plot are the phase space density of the ions and the dashed curves show, in arbitrary units, the ion number density in the velocity-space bins (proportional to  $v^2 F(v)$ ).

Fig. 3. Contour plot of the water group ion velocity-space distribution obtained over a 5-min averaging period centered at 2327:39 UT ( $D = 1.46 \times 10^5$  km), taken from *Goldstein et al.* [1992]. (Note that the upstream field-aligned velocities are along  $+v_{\parallel}$  in this plot.). New pickup ions are injected at the position of the cross. The superimposed dashed curve which passes through the cross shows the bispherical scattering geometry for the local Alfvén speed  $V_A = 5.6$  km/s.

Fig. 4. Details of the bispherical shell portion radii and injection angles used to calculate  $\langle |v| \rangle_{inj}$  in the water group ion bulk velocity frame.

Fig. 5. Variation of the theoretical  $\langle |v| \rangle_{inj}$  with  $\alpha$ , for various ratios of  $V_A/u_{wg}$ . The  $\langle |v| \rangle_{inj}$  is expressed as a ratio to the original injection at  $|u_{wg}|$ .

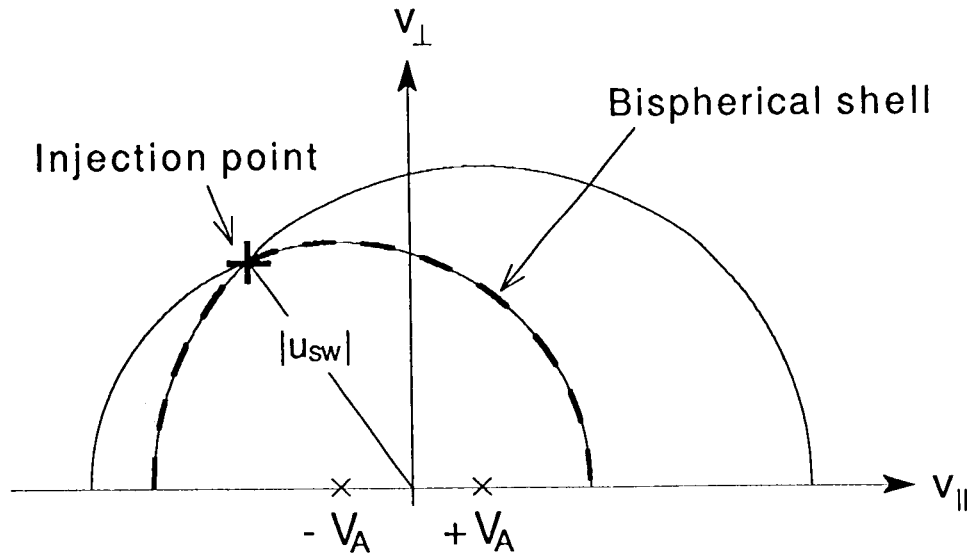


Fig. 1. Sketch of the theoretical bispherical shell geometry for implanted cometary ions in the solar wind frame, where  $v_{||}$  and  $v_{\perp}$  are the field-aligned and perpendicular (gyrating) velocities, respectively. The shell comprises the low energy portions of the ion paths about the scattering centers of the upstream and downstream propagating Alfvén waves,  $-V_A$  and  $+V_A$ , respectively.

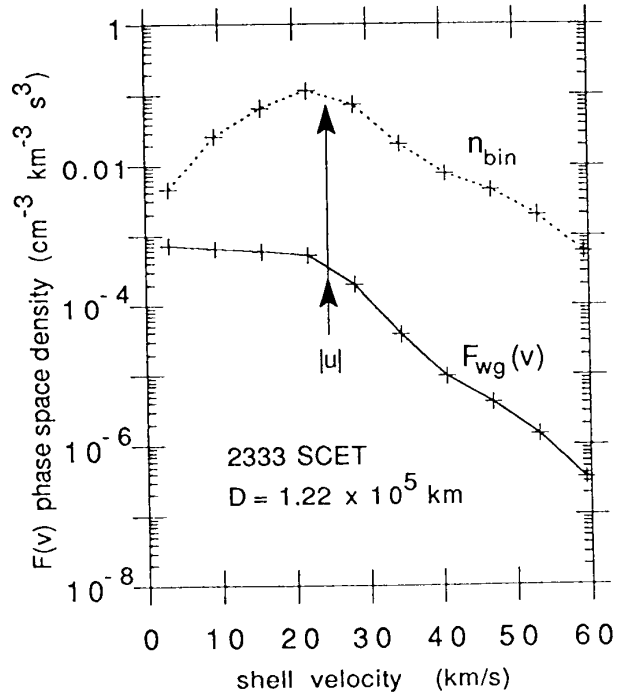
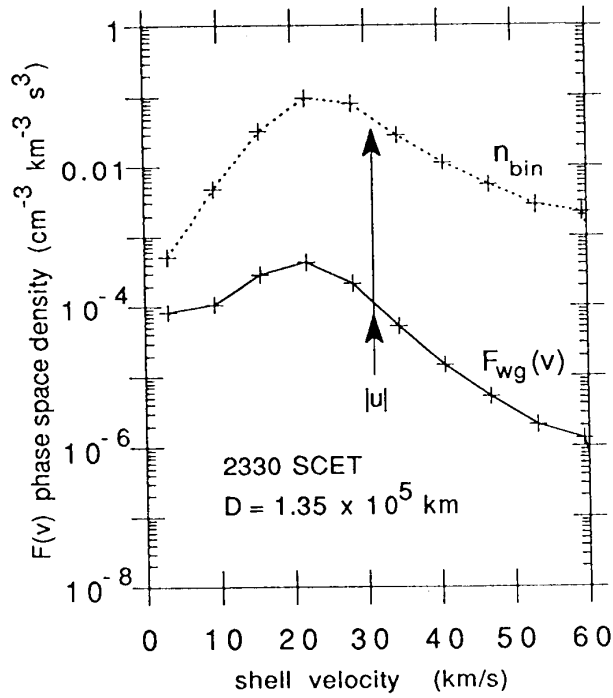
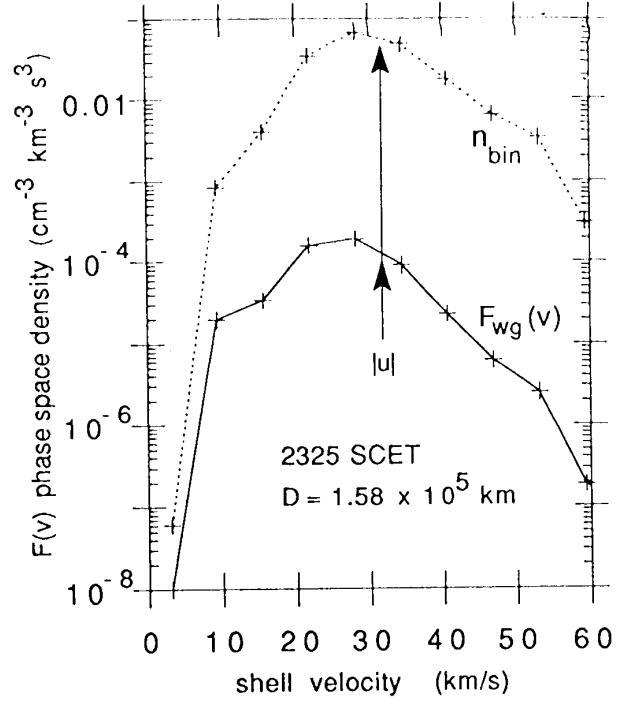
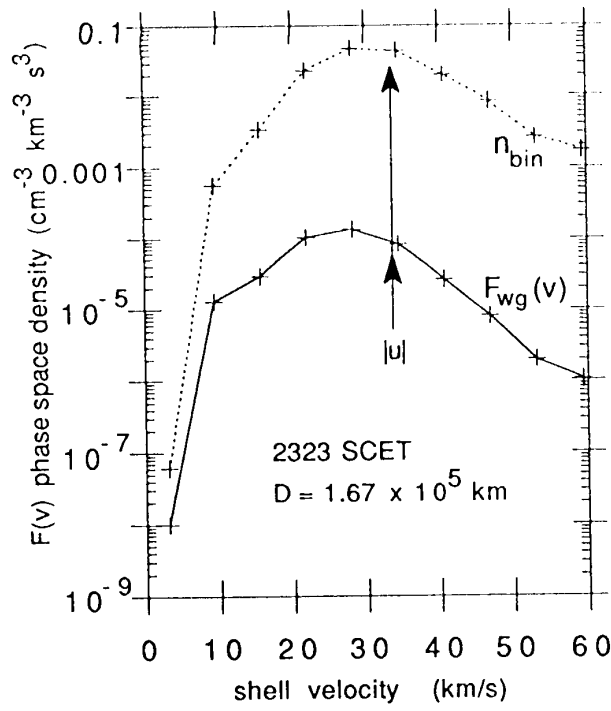


Fig. 2. Examples of the cometary water-group ion distributions observed by the Giotto Ion Mass Spectrometer. The solid curves in each plot are the phase space density of the ions and the dashed curves show, in arbitrary units, the ion number density in the velocity-space bins (proportional to  $v^2 F(v)$ ).

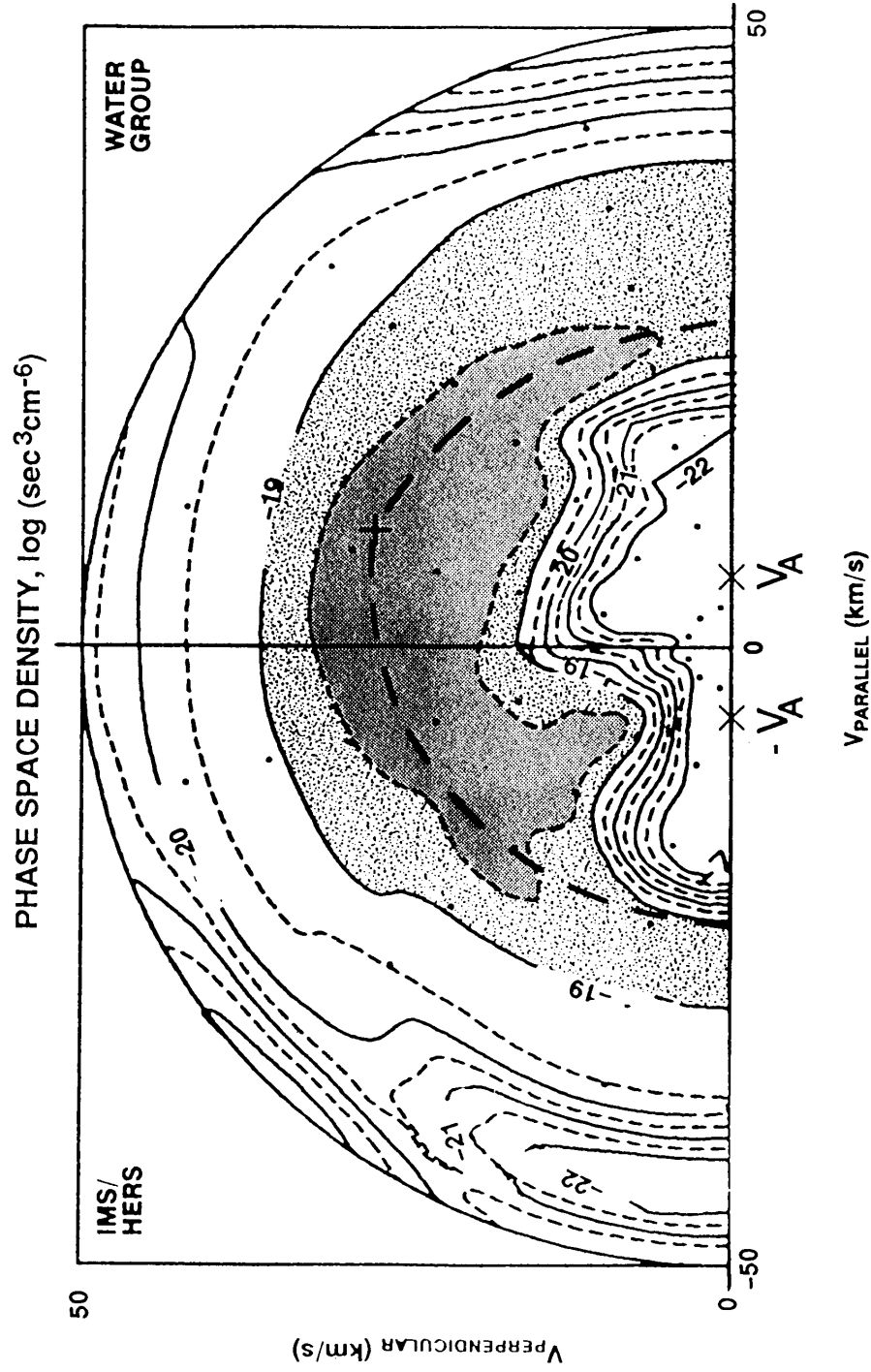


Fig. 3. Contour plot of the water group ion velocity-space distribution obtained over a 5-min averaging period centered at 2327:39 UT ( $D = 1.46 \times 10^5$  km), taken from *Goldstein et al.* [1992]. (Note that the upstream field-aligned velocities are along  $+v_{\parallel}$  in this plot.). New pickup ions are injected at the position of the cross. The superimposed dashed curve which passes through the cross shows the bispherical scattering geometry for the local Alfvén speed  $V_A = 5.6$  km/s.



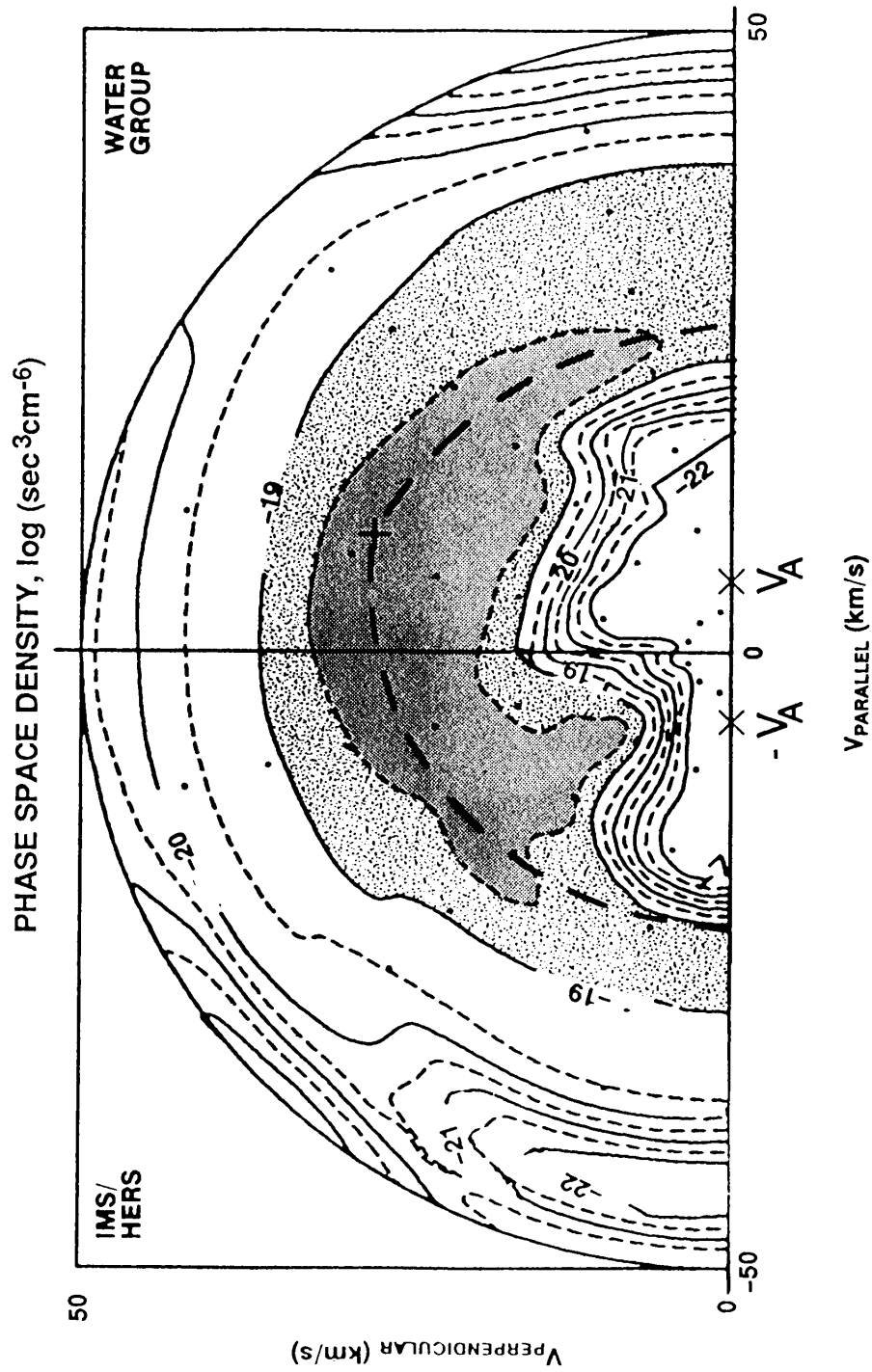


Fig. 3. Contour plot of the water group ion velocity-space distribution obtained over a 5-min averaging period centered at 2327:39 UT ( $D = 1.46 \times 10^5$  km), taken from *Goldstein et al.* [1992]. (Note that the upstream field-aligned velocities are along  $+v_{\parallel}$  in this plot.). New pickup ions are injected at the position of the cross. The superimposed dashed curve which passes through the cross shows the bispherical scattering geometry for the local Alfvén speed  $V_A = 5.6$  km/s.

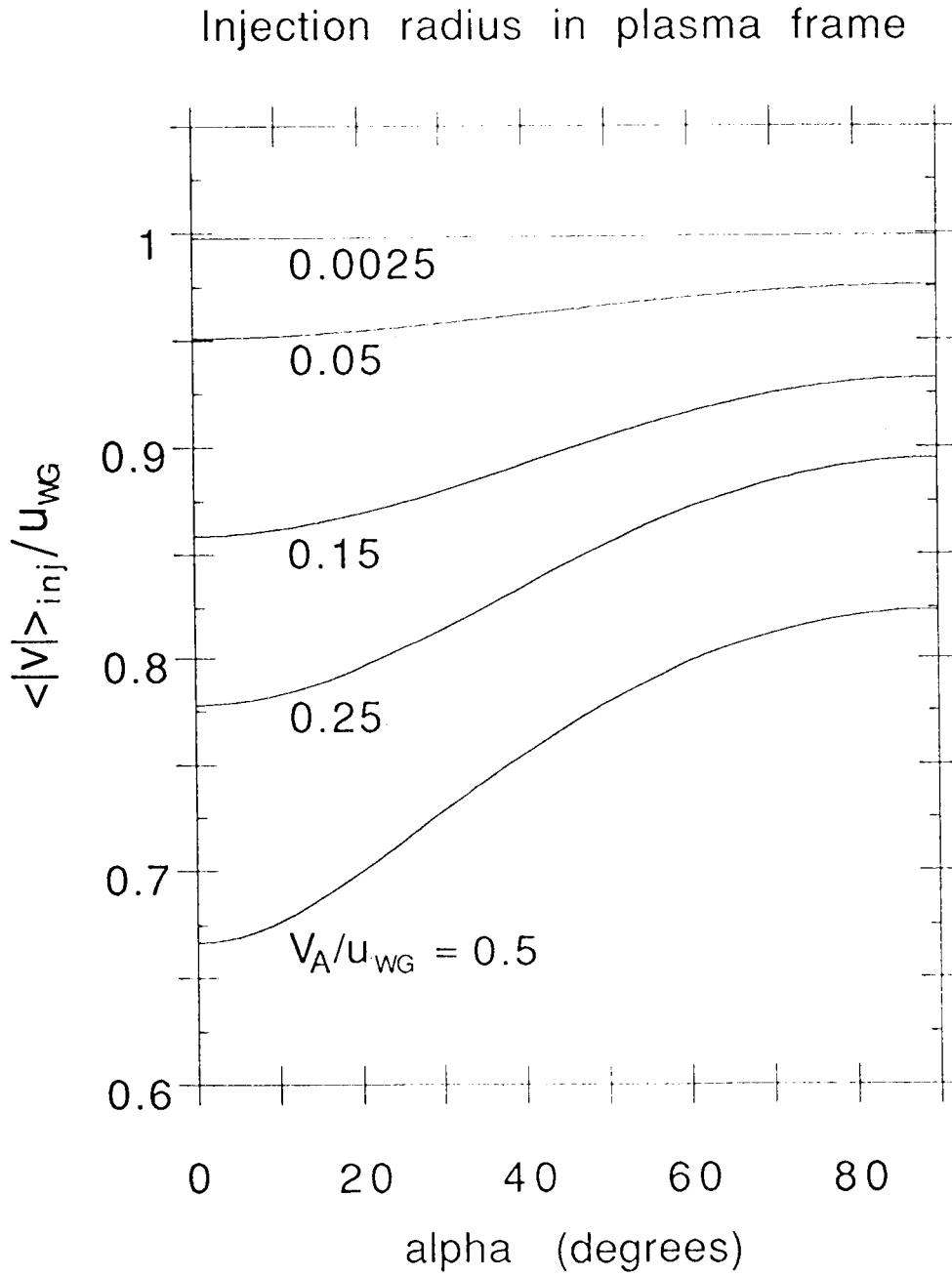


Fig. 5. Variation of the theoretical  $\langle |v| \rangle_{inj}$  with  $\alpha$ , for various ratios of  $V_A / u_{wg}$ . The  $\langle |v| \rangle_{inj}$  is expressed as a ratio to the original injection at  $|u_{wg}|$ .